# Fabrication of a Nanosize Hematite Pigment via Waste Ferrous Sulfate Recycling Using Sulfur Reduction

Wang, Ye; Ren, Genkuan; Jiang, Bing; Yang, Lin; Zhang, Zhiye; Wang, Xinlong; Zhong, Yanjun; Chen, Zhiyuan; Yang, Xiushan; Morita, Kazuki

**DOI**
10.1007/s11663-022-02584-5

**Publication date**
2022

**Document Version**
Final published version

**Published in**
Metallurgical and Materials Transactions B: Process Metallurgy and Materials Processing Science

# Fabrication of a Nanosize Hematite Pigment *via* Waste Ferrous Sulfate Recycling Using Sulfur Reduction

YE WANG, GENKUAN REN, BING JIANG, LIN YANG, ZHIYE ZHANG, XINLONG WANG, YANJUN ZHONG, ZHIYUAN CHEN, XIUSHAN YANG, KAZUKI MORITA, and WENHUI MA

Nanometer-sized hematite was prepared *via* a two-step process. In the first step, $FeSO_4 \cdot 7H_2O$ was oxidized to $Fe_2(SO_4)_3$ by oxygen in an acidic solution. In the second step, the $Fe_2(SO_4)_3$ was reduced to nanosize hematite with sulfur vapor at 550 °C. The hematite has good thermal requirements of the international standard ISO 1248-A-I-1-a for an iron oxide red pigment.

YE WANG, BING JIANG, LIN YANG, ZHIYE ZHANG, XINLONG WANG, and YANJUN ZHONG are with the School of Chemical Engineering, Sichuan University, Chengdu, 610065, P.R. China. GENKUAN REN is with the College of Chemistry and Chemical Engineering, Yibin University, Yibin, 64000, P.R. China. ZHIYUAN CHEN is with the Department of Materials Science and Engineering, Delft University of Technology, Mekelweg 2, 2628 CD Delft, The Netherlands. XIUSHAN YANG is with the School of Chemical Engineering, Sichuan University, and also with the College of Chemical Engineering, Sichuan University, No 24, South 1th Section, 1st Ring Road, Chengdu, Sichuan, 610065, P.R. China. Contact e-mail: 331223839@qq.com KAZUKI MORITA is with the Department of Material Engineering, The University of Tokyo, Tokyo, 113-8656, Japan. WENHUI MA is with the Kunming University of Science and Technology, Beijing, 650031, Yunnan, P.R. China

Manuscript submitted July 22, 2021; accepted June 14, 2022.



Published online: 13 December 2022

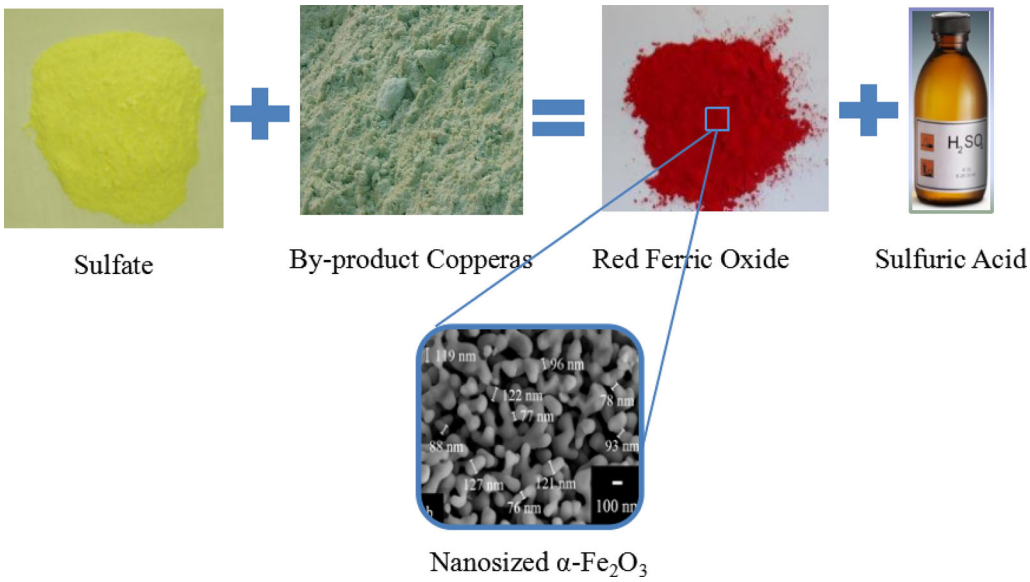


https://doi.org/10.1007/s11663-022-02584-5


FERROUS sulfate ($FeSO_4 \cdot 7H_2O$), a by-product from titanium dioxide production, is considered as a waste. Heaps of this material are piled up in mountain which not only causes the waste of resources but also results in environmental pollution. Therefore, the comprehensive utilization of waste ferrous sulfate has become a hot topic of current research. Presently, there are three main applications for the waste ferrous sulfate. First, the poly-ferric sulfate as a coagulant can be prepared,[1] but the low market demand restricts its development. Second, mixed combustion with pyrite to produce sulfuric acid is another important means to utilize $FeSO_4 \cdot 7H_2O$. However, the low economic efficiency cannot be ignored given that sulfuric acid is inexpensive. Third, the waste ferrous sulfate is used to produce pigments including magnetite ($Fe_3O_4$),[2] maghemite ($\gamma$-$Fe_2O_3$),[3] and hematite ($\alpha$-$Fe_2O_3$).[4]

Hematite is an important form of iron oxide in nature. The nanometer-sized hematite has been widely applied in biomedicine,[5] pollution control,[6] and photocatalytic reaction[7,8] because of its unique physical properties.[9] Hence, many researchers have been focusing remarkable efforts on developing effective and low-cost methods for producing hematite nanoparticles.[10] Currently, the chemical precipitation method,[3] the sol-gel method,[11] and the hydrothermal method[12] are the main methods to prepare hematite nanoparticles. For example, hematite nanoparticles were produced from $FeSO_4 \cdot 7H_2O$ *via* a hydrothermal-annealing method[13] or a surfactant-mediated co-precipitation method.[14] However, the aforementioned methods are limited in industrial applications due to the complexity of the process and high energy consumption. In this study, sulfur reduction reaction, as a simple, large-scale, and low-cost method, is proposed to produce nanosize hematite particles. Simultaneously, the released $SO_2$ from reaction process was used to produce sulfuric acid to reduce production costs and energy consumption. In the proposed process, $FeSO_4 \cdot 7H_2O$ was firstly oxidized to $Fe_2(SO_4)_3$ by oxygen in an acidic solution. In the next step, the purified $Fe_2(SO_4)_3$ prepared by crystallization was reduced with sulfur to produce the nanosize hematite (93.5 pct) and produced $H_2SO_4$.

The nanometer-sized hematite was prepared by sulfur reduction method using system I ($Fe_2(SO_4)_3 + S$), or system II ($FeSO_4 + S$) as the starting materials,l which system is determined by thermodynamics analysis. The equilibrium compositions of the reaction systems were calculated at different temperatures by HSC 7.0, and the results are displayed in Figure 1.

Figure 1(a) illustrates that the decomposition temperature of $Fe_2(SO_4)_3$ for system I is about 300 °C. Only the small amount of $Fe_3O_4$ is generated when the temperature reaches 800 °C. Therefore, the major products are $Fe_2O_3$ and $SO_2$ between 300 °C and approximately 800 °C. Thus, it can be inferred that the main reaction in system *I* is Eq. [1]. Figure 1(b) shows that the decomposition temperature of $FeSO_4$ begins at 450 °C and finishes by 800 °C. It can be seen that the decomposition temperature of $FeSO_4$ is higher than that of $Fe_2(SO_4)_3$, and it is evident that both $Fe_2O_3$ and $Fe_3O_4$ are generated between 300 °C and 800 °C. Thus, it can be inferred that the main reactions in system *II* are Eqs. [2] and [3].

$$2Fe_2(SO_4)_3 + 3S = 2Fe_2O_3 + 9SO_2(g), \quad [1]$$

$$\Delta G_1^0 = -1.61\ T + 376\ \text{kJ} \cdot \text{mol}^{-1},$$

$$4FeSO_4 + S = 2Fe_2O_3 + 5SO_2(g), \quad [2]$$

$$\Delta G_1^0 = -0.85\ T + 332\ \text{kJ} \cdot \text{mol}^{-1},$$

$$3FeSO_4 + S = Fe_3O_4 + 4SO_2(g), \quad [3]$$

$$\Delta G_1^0 = -0.71\ T + 275\ \text{kJ} \cdot \text{mol}^{-1}.$$

Above all, the completion temperature of system *I* (500 °C) is lower than that of system *II* (800 °C). In addition, the main solid product of system *I* is $Fe_2O_3$, whereas both of $Fe_2O_3$ and $Fe_3O_4$ are generated in system *II*. Therefore, system *I* is superior to system *II* for the preparation of hematite. That is to say, $FeSO_4 \cdot 7H_2O$ is firstly oxidized to $Fe_2(SO_4)_3$ by oxygen in sulfuric acid solution, and then nanometer-sized hematite is prepared by reducing $Fe_2(SO_4)_3$ with S (system *I*).

The sulfur (99 pct) and waste ferrous sulfate were obtained from Sichuan Hongda Group. The components of waste ferrous sulfate are listed in Table I.

The nanometer-sized hematite was produced by a combination of oxygen oxidation process and sulfur vapor reduction reaction using waste ferrous sulfate and sulfur as the starting materials. First, waste ferrous sulfate was dissolved in sulfuric acid solution (0.1 mg/L), and insoluble matter was filtered out. Subsequently, ferrous sulfate was oxidized to $Fe_2(SO_4)_3$ by oxygen at 80 °C for 90 minutes (Eq. [4]).

$$4FeSO_4 \cdot 7H_2O + O_2 + 2H_2SO_4 = 2Fe_2(SO_4)_3 + 30H_2O. \quad [4]$$

The crystallized ferric sulfate ($Fe_2(SO_4)_3$, 99.0 pct) was separated from mother liquor and then dried at 105 °C for 300 minutes. Second, the mixture of ferric sulfate with sulfur at the ratio of 6:1 was evenly ground with omnidirectional planetary ball mill for 30 minutes and then placed in porcelain boat. After that, the porcelain boat was put into the high-temperature zone of atmosphere tube furnace, and ferric sulfate reacted with the formed sulfur vapor for 60 minutes at 550 °C under nitrogen protection (Eq. [1]). The calcined product was cooled to room temperature in the furnace. The obtained product was washed with deionized water and absolute ethanol for several times. Finally, the resulting nanometer-sized hematite pigment was dried at

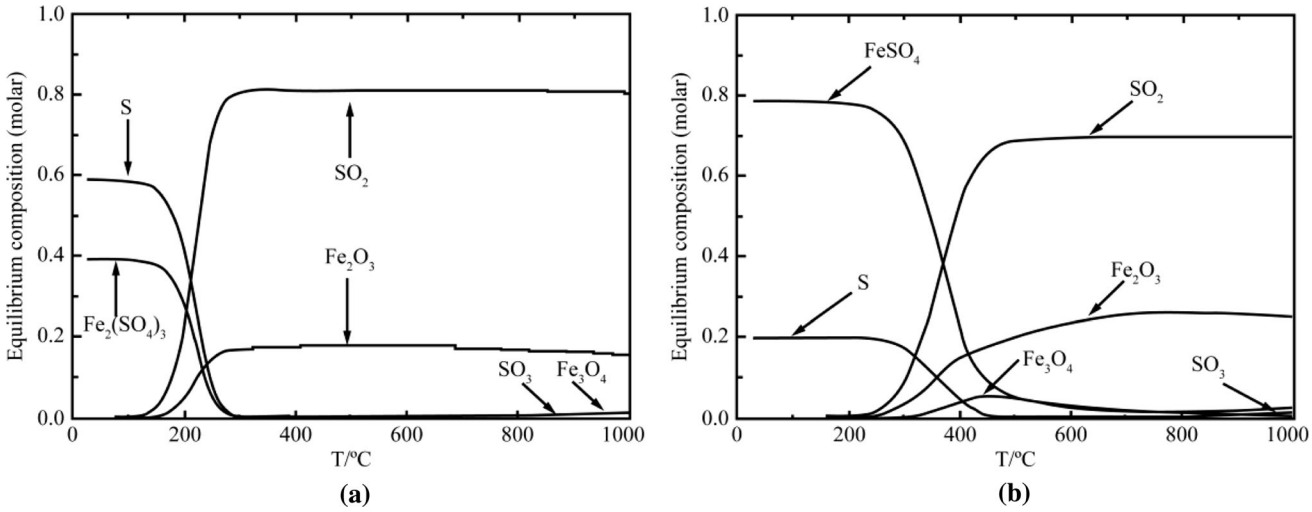


Fig. 1—Equilibrium composition of (*a*) S-$Fe_2(SO_4)_3$ reaction system (*I*), and (*b*) S-$FeSO_4$ reaction system (*II*).

**Table I. Components of Waste Ferrous Sulfate**

| Ingredient | Mass Content (Percent) | Ingredient | Mass Content (Percent) |
|---|---|---|---|
| $FeSO_4 \cdot 7H_2O$ | 90.01 | $CaSO_4 \cdot 2H_2O$ | 0.38 |
| $MgSO_4 \cdot 7H_2O$ | 3.94 | $TiOSO_4$ | 0.30 |
| $MnSO_4 \cdot 5H_2O$ | 1.22 | insoluble impurities | 3.24 |
| $Al_2(SO_4)_3 \cdot 18H_2O$ | 0.60 | others | 0.31 |

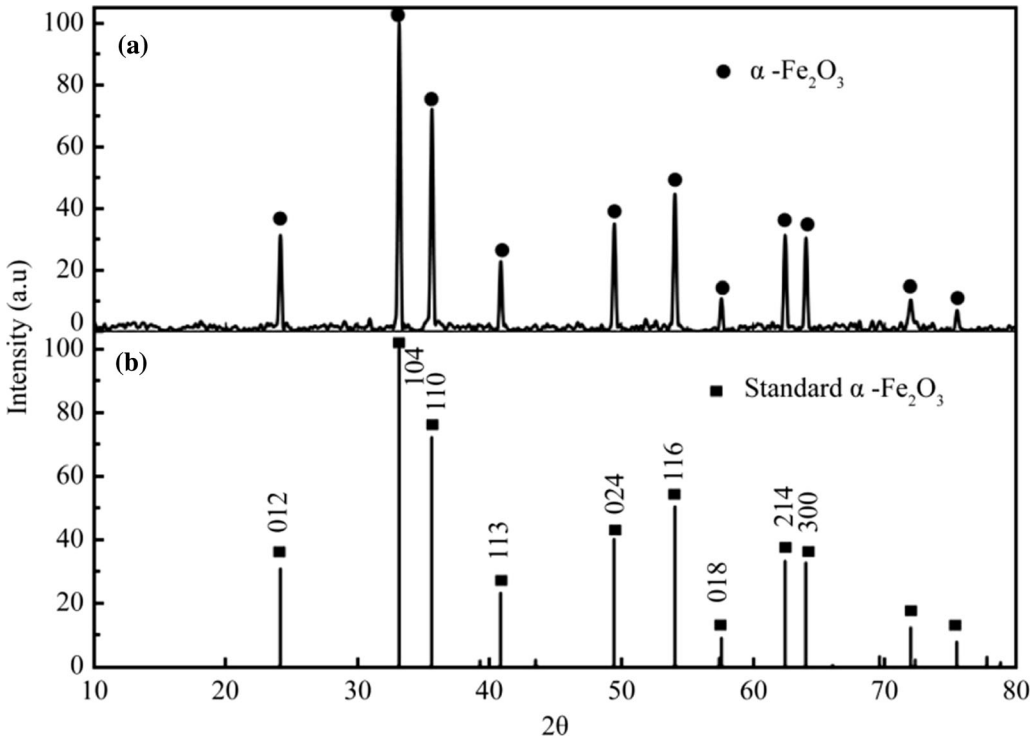


Fig. 2—The XRD patterns of the as-obtained samples and standard hematite.

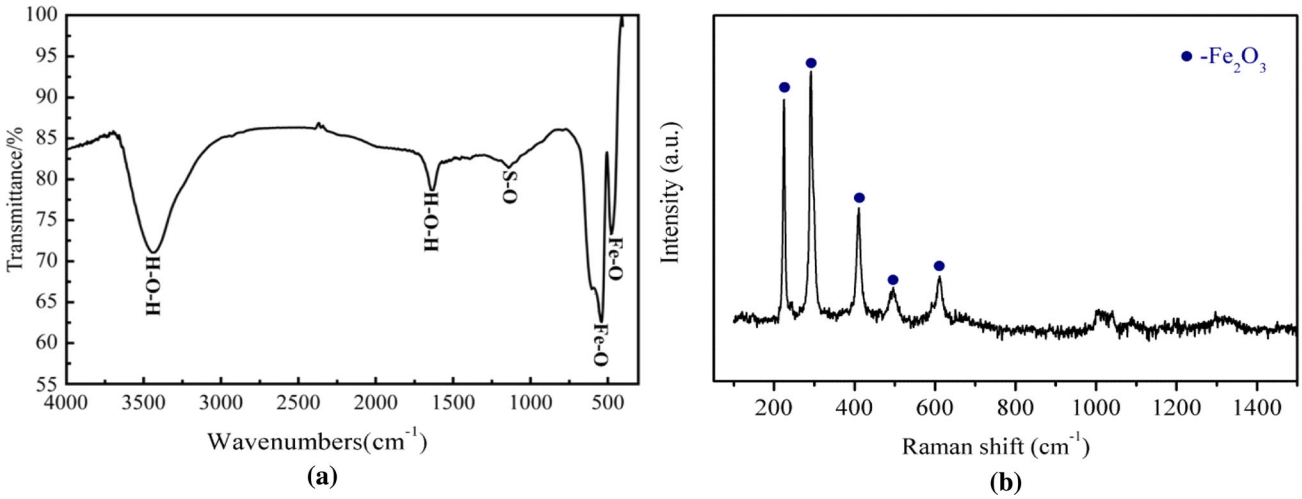


Fig. 3—(*a*) FTIR spectrum and (*b*) Raman spectrum of the nanometer-sized hematite pigment.

80 °C in an air oven. Meantime, water solution was used to absorb the $SO_2$ produced in reaction process.

The X-ray diffraction (XRD) was used for phase characterization on a Bruker D8 X-ray diffractometer using Cu-K$\alpha$ radiation ($\lambda$ = 1.5408 Å)at 50 mA and 40 kV at the scattering angles ($2\theta$) ranged from 10 to 80 deg. The morphology of the sample was examined using JEOL JSM 7500F scanning electron microscopy (FESEM) at an accelerating voltage of 20 kV. The surface functional groups of the sample were determined by Fourier-transform infrared spectroscopy (FTIR, Avatar370, Thermo Nicolet 6700) with the KBr pellet technique in the range of 400–4000 $cm^{-1}$. Raman spectroscopy was done on a dispersive micro-Raman spectrometer (LabRAM HR, Horiba) equipped with a 732 nm laser. The chemical state of the sample was analyzed using X-ray photoelectron spectroscopy (XPS, Kratos, XSAM800) with an AlK$\alpha$ X-ray source with binding energy calibrated by C 1s line at 284.6 eV. Thermogravimetric-differential scanning calorimeter (TG-DSC, NETZSCH) was used to determine the thermal stability of the sample under nitrogen flow (20 $ml{\cdot}min^{-1}$ ) at the temperature range of 35–800 °C at a heating rate of 20 °C·$min^{-1}$. Zeta potential under different pH values was determined with a Malvern brand analyzer (Zetasizer Nano, ZS90).

The XRD patterns of the resulting sample and standard hematite (JCPDS No. 33-0664) are shown in Figure 2. As seen in Figure 2, the characteristic peaks of the sample match well with those of the standard hematite, and no other impurity peaks are observed, indicating that the as-formed material is composed of the pure hematite with the rhombohedral crystal system.[15] The crystallite size estimated from the broadening of the peak corresponding to 104 diffraction of hematite is 50 nm using the Debye–Scherrer formula.[16]

To find out the surface functional groups of the nanometer-sized hematite pigment, the resulting nanometer-sized hematite pigment was analyzed by the FTIR spectrum and Raman spectrum, and the results are depicted in Figure 3. From Figure 3(a), the absorption peaks observed at 1632 and 3437 $cm^{-1}$ can be assigned to the H-O-H bending and stretching vibration due to adsorbing water molecules on the surface of hematite, whereas the characteristic band at 1138 $cm^{-1}$ can be attributed to the stretching vibration of $SO_4^{2-}$ from unreacted sulfate.[17] In addition, the remarkable bands at 538 $cm^{-1}$ and 472 $cm^{-1}$ can be assigned to $Fe^{3+}$-O and $Fe^{2+}$-O in hematite,[18] suggesting the fabrication of nanometer-sized hematite. From Figure 3(b), the significant bands located at 225 $cm^{-1}$ and 496 $cm^{-1}$ can be assigned to the Fe-O stretching vibrational modes, and the peaks observed at 292 $cm^{-1}$, 411 $cm^{-1}$, and 611 $cm^{-1}$ are corresponded to the symmetric bending modes, which are consistent with the characteristic peaks of hematite reported in the literature.[19,20] The result further confirms that the as-formed sample is the nanometer-sized hematite pigment, which is agreement well with the result obtained from XRD analysis.

The SEM image of the resultant hematite is displayed in Figure 4. As demonstrated in Figure 4, the nanometer-sized hematite is composed of spherical particles. The nanometer-sized hematite has a uniform distribution and no agglomeration. According to particle size distribution, the prepared sample has an average diameter of ~ 59 nm, which is similar to the crystallite size determined by XRD.

The oxidation state of iron in the sample was analyzed by the X-ray photoelectron spectroscopy (XPS). Figure 5 shows the XPS wide-scan and Fe2p spectra for the prepared hematite. The three main peaks at 710.52, 530.50, and 284.52 eV are mainly composed of iron and oxygen elements with Fe2p, O1s, and C1s core-level spectra[21] in Figure 5(b), and the two peaks at 710.7 and 724.4 eV are agreement with Fe $2p_{3/2}$ and Fe $2p_{1/2}$ in accordance with the reported results.[22] It demonstrates the formation of the nanometer-sized hematite by the reduction of $Fe_2(SO_4)_3$ with S. The satellite peak at the binding energy of 718.8 eV is the characteristic of the hematite, further verifying the formation of hematite.[23]

The total weight loss of 15.54 pct was analyzed by TG-DSC as shown in Figure 6. The observed peak at 93.26 °C can be assigned to desorption of surface

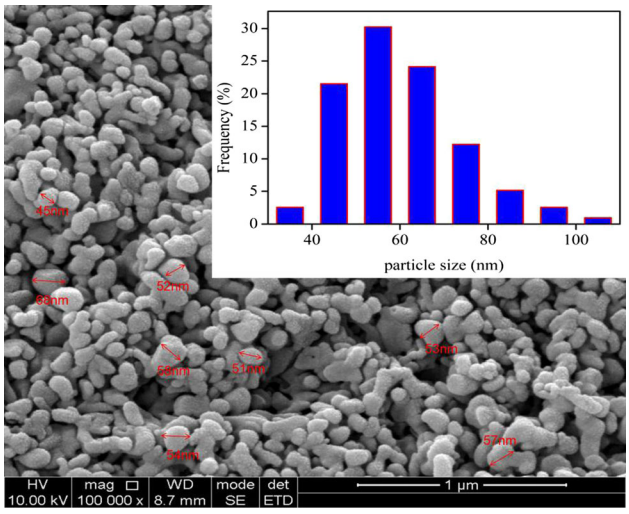


Fig. 4—SEM image of the nanometer-sized hematite pigment (Inset: particle size distribution).

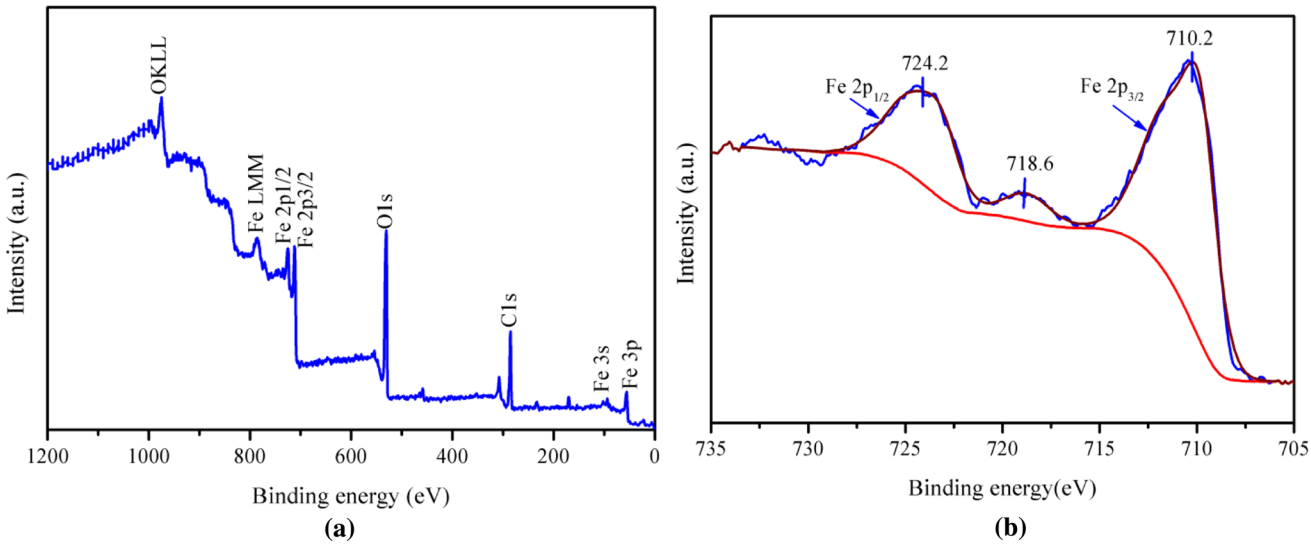


Fig. 5—XPS of **(a)** wide-scan spectrum and (*b*) Fe2p spectrum for the as-formed nanometer-sized hematite.

adsorbed water on hematite with weight loss of 8.70 pct. Waste ferrous sulfate from titanium dioxide industry is consisted of different sulfates. Some sulfates (*e.g.*, $MgSO_4$, $MnSO_4$, $Al_2(SO_4)_3$) remain original state at experiment temperature due to different reaction temperatures between different sulfate and sulfur. The small peak at 589.42 °C can be attributed to decomposition of unreacted sulfate. Accordingly, the nanometer-sized hematite has good thermal stability without reaction at 500 °C.

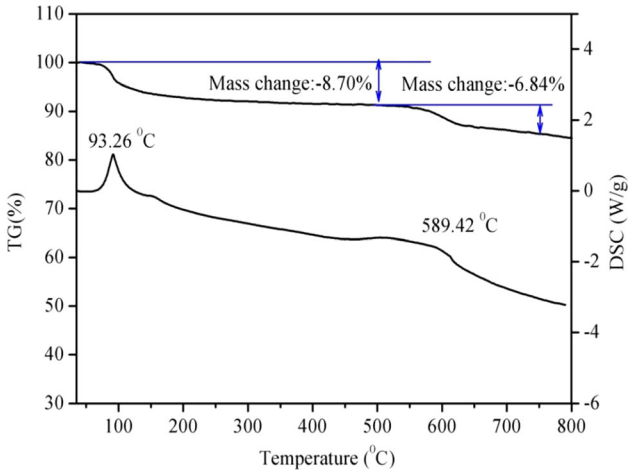


Fig. 6—TG-DSC curve for the as-formed nanometer-sized hematite.

To analyze colloid stability in water-based paint, Zeta potentials under different pH value are measured at room temperature at the concentration of 0.1 pct. Zeta potentials are plotted against solution pH value as seen in Figure 7. It shows that the pH value at point of zero charge ($pH_{PZC}$) is 8.8. The nanosize hematite is positively charge below $pH_{PZC}$ and negatively charged above $pH_{PZC}$. The nanosize hematite has good dispersion in water-based paint for the negative Zeta potential.

Colorimetric measurement of the obtained nanometer-sized hematite pigment was performed, and the results are shown in Table II. $a^*$ value in the positive direction is corresponded to red chromaticity, while $b^*$ value is assigned to the yellow chromaticity. The positive $a^*$ coordinate value and negative $b^*$ coordinate value indicate that the color tone is a better red. The prepared nanometer-sized hematite pigment should be red when the hue is closed to zero.

A effective process to prepare nanosize hematite by the recycling of waste ferrous sulfate has been successfully developed with sulfur reduction technique. The synthetic process consisted oxidation of ferrous sulfate and the reduction of ferric sulfate were investigated by

**Table II. Color coordinates and Hue of the As-prepared Nanometer-Sized Hematite Pigment**

| Color Coordinate | $L$ | $a^*$ | $b^*$ | Hue |
|---|---|---|---|---|
| Hematite pigment | 6.76 | 5.6908 | − 0.6892 | − 23.33 |

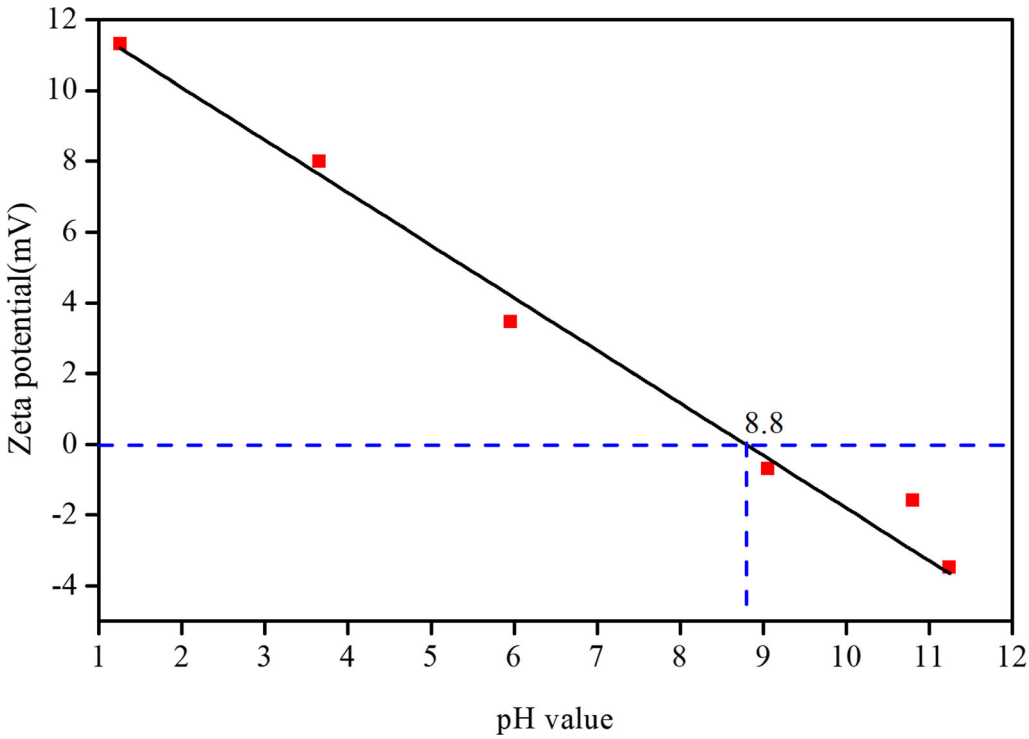


Fig. 7—Effect of pH value on zeta potential for hematite.

the thermodynamic analysis, and suitable condition is obtained for the reduction of ferric sulfate. Under optimum condition, the as-formed nanometer-sized hematite has an average diameter of ~ 59 nm. The obtained nanometer-sized hematite has good thermal stability below 500 °C and good dispersion in water-based paint. The nanometer-sized hematite synthesized by using waste ferrous sulfate as a starting material effectively reduces cost production and environmental pollution pressure.

## ACKNOWLEDGMENTS

This research was performed with the support of the Technology Cooperation Program of Sichuan University and Panzhihua City (2021CDPZH-3), the Science and technique Department of Sichuan Province (22YFS0461) and the National Natural Science Foundation of China (No. 22072096). The authors also thank the SEM imaging measurements by the Engineering Teaching Center, School of Chemical Engineering, Sichuan University.

## CONFLICT OF INTEREST

The corresponding author declares that there is no conflict of interest on behalf of all authors.

## REFERENCES

1. D. Jia, M. Li, G. Liu, P. Wu, J. Yang, Y. Li, S. Zhong, and W. Xu: *Colloids Surf., A*, 2017, vol. 512, pp. 111–17.
2. G. Ren, X. Wang, Z. Zhang, B. Zhong, L. Yang, and X. Yang: *Dyes Pigments*, 2017, vol. 147, pp. 24–30.
3. S. Babay, T. Mhiri, and M. Toumi: *J Mol Struct*, 2015, vol. 1085, pp. 286–93.
4. X. Li, C. Wang, Y. Zeng, P. Li, T. Xie, and Y. Zhang: *J Hazard Mater*, 2016, vol. 317, pp. 563–69.
5. Y. Xu, S. Yang, G. Zhang, Y. Sun, D. Gao, and Y. Sun: *Mater Lett*, 2011, vol. 65, pp. 1911–14.
6. W. Gao, J. Yan, L. Qian, L. Han, and M. Chen: *Environ. Technol. Innov.*, 2018, vol. 9, pp. 82–90.
7. S.G. Hosseini and E. Ayoman: *J. Therm. Anal. Calorim.*, 2017, vol. 128, pp. 915–24.
8. B. Alqasem, N. Yahya, S. Qureshi, M. Irfan, Z.U. Rehman, and H. Soleimani: *Mater. Sci. Eng. B*, 2017, vol. 217, pp. 49–62.
9. J. Štajdohar, M. Ristić, and S. Musić: *J. Alloy Compds.*, 2012, vol. 532, pp. 41–8.
10. E. Darezereshki: *Mater. Lett.*, 2010, vol. 64, pp. 1471–72.
11. H. Liang, K. Liu, and Y. Ni: *Mater. Lett.*, 2015, vol. 159, pp. 218–20.
12. A. Benhammada, D. Trache, M. Kesraoui, et al.: *Thermochim. Acta*, 2020, vol. 686, pp. 1–1.
13. Q. Qin, X. Zhu, and X. Zhang: *Mater. Sci. Eng. B*, 2022, vol. 275, pp. 1–6.
14. N. Gupta, Y. Ghaffari, J. Bae, et al.: *J. Mol. Lio*, 2020, vol. 301, pp. 1–9.
15. A. Rufus, N. Sreeju, V. Vilas, and D. Philip: *J. Mol. Liq.*, 2017, vol. 242, pp. 537–49.
16. Y. Shen, X. Li, Q. Zhao, et al.: *Mater. Res. Bull.*, 2011, vol. 46, pp. 2235–39.
17. Y. Wei, X. Dong, A. Ding, and D. Xie: *J. Taiwan Inst. Chem. E*, 2016, vol. 58, pp. 351–56.
18. M. Tadic, M. Panjan, V. Damnjanovic, and I. Milosevic: *Appl. Surf. Sci.*, 2014, vol. 320, pp. 183–87.
19. B. Ahmmad, K. Leonard, M.S. Islam, J. Kurawaki, M. Muruganandham, T. Ohkubo, and Y. Kuroda: *Adv. Powder. Technol.*, 2013, vol. 24, pp. 160–67.
20. Y.Y. Xu, D. Zhao, X.J. Zhang, W.T. Jin, P. Kashkarov, and H. Zhang: *Physica E*, 2009, vol. 41, pp. 806–11.
21. K. Bindu, K.M. Ajith, and H.S. Nagaraja: *J. Alloy Compds.*, 2018, vol. 735, pp. 847–45.
22. J. Zhao, J. Brugger, and A. Pring: *Geosci. Front*, 2019, vol. 10, pp. 29–41.
23. R. Al-Gaashani, S. Radiman, N. Tabet, and A.R. Daud: *J. Alloy Compds.*, 2013, vol. 550, pp. 395–401.